J. Plasma Physics (2004), *vol.* 70, *part* 5, *pp.* 613–623.
DOI: 10.1017/S0022377804002892 Printed in the United Kingdom

Low-frequency instabilities due to energetic oxygen ions

S. V. SINGH, A. P. KAKAD, R. V. REDDY and G. S. LAKHINA

Indian Institute of Geomagnetism, Plot No. 5, Sector-18, New Panvel (W), Navi Mumbai-410218, India
(satyavir@iigs.iigm.res.in)

(Received 5 August 2003, revised 12 December 2003 and accepted 27 December 2003)

Abstract. Low-frequency instabilities excited by energetic oxygen ions are investigated. The model consists of Maxwellian distributions for electrons and protons and Dory–Guest–Harris loss-cone distribution for oxygen ions. The electrons and protons are treated as magnetized and oxygen ions as unmagnetized. The response of the electrons is fully electromagnetic and that of the protons and oxygen ions is electrostatic. A possible application of the investigation to space plasmas is pointed out.

1. Introduction

Protons and other energetic heavy ions, such as helium and oxygen, have been important constituents of laboratory as well as space plasmas. The energetic particles arise naturally in the radio-frequency (RF) heating of plasmas and laser fusion. The free energy provided by the energetic particles can excite plasma instabilities (Watkins 1998; Putvinski 1998) and there is a subsequent loss of fast particles by steady state diffusion or rapid expulsion. In space plasmas, the AMPTE/CCE spacecraft frequently observed electromagnetic ion cyclotron (EMIC) waves in the outer magnetosphere beyond $L = 7$ (Anderson et al. 1990, 1992a, b); L is the McIlwain parameter and it represents the equatorial crossing distance of a line of force. The wave spectral properties and frequency of occurrence depends on local time and can be explained by the resonant instability of anisotropic ring current H^+ ions in the variable background thermal plasma (Horne and Thorne 1993, 1994).

In the ring current region, oxygen ions (O^+) of ionospheric origin are an important constituent and during the geomagnetic quiet periods the fractional concentration of the energetic oxygen ions is low (below 10%). However, during the main phase of the storm, the energy content of the geomagnetically trapped particles increases and the fractional concentration of the oxygen ions is also enhanced. It can reach a value in excess of hydrogen ions for the largest magnetic storms. Recent observations have shown the correlation between the minimum value of the disturbance storm time (Dst) index and the fractional concentration of oxygen ions (Hamilton et al. 1988; Daglis et al. 1994, 2000; Daglis, 1997; Nose et al. 2001). The Dst index is commonly used for measuring the intensity of a magnetic storm and it acts as a proxy for the energy contents of the storm time ring current. The process of injection of the oxygen ions of ionospheric origin into the ring current region

of the magnetosphere and their acceleration to higher energies could involve either perpendicular heating leading to the generation of ion conics (Sharp et al. 1977; Gorney et al. 1981) or field aligned currents associated with potential drops between the ionosphere and magnetosphere (Shelly et al. 1976; Peterson et al. 1993). Geotail spacecraft observed oxygen ions in the near-Earth plasma sheet region during the substorm expansion phase (Nose et al. 2000). Energetic oxygen ions of ionospheric origin with hundreds of keV energies have been observed in the cusp region by the POLAR satellite (Chen and Fritz 2001). The presence of oxygen ions during the storms can affect the excitation of low-frequency instabilities such as EMIC instability. Thorne and Horne (1994) showed that during the geomagnetic storms when the oxygen ion content is significantly enhanced, the absorption of EMIC waves becomes efficient and may lead to the acceleration of O^+ ions of ionospheric origin to ring current energies. Horne and Thorne (1994) studied the convective instabilities of the EMIC waves in the outer magnetosphere and discussed that the waves below the cyclotron frequency of the helium (He^+) ions are not reflected when the O^+ ion concentration is small.

Several spacecraft, namely OGO 3, IMP 6, S3-3, GEOS 1 and 2, Viking etc., have observed the low-frequency waves with frequencies from a few Hz to a few kHz (Russell et al. 1970; Anderson and Gurnett 1973; Gurnett 1976; Gurnett and Frank 1977, 1978; Perraut et al. 1982; Laakso et al. 1990). These waves can be excited by the energetic proton or ion distributions. In the ring current region, a quasi-electrostatic instability can be excited by the loss-cone distribution of protons (Coroniti et al. 1972; Bernstein et al. 1974; Lakhina 1976; Bhatia and Lakhina 1980). Recently, Thorne and Horne (1997) studied the modulation of EMIC instability due to the interaction with ring current O^+ ions during geomagnetic storms. They demonstrated that during a modest storm, strong EMIC excitation can occur in the frequency band above the oxygen gyrofrequency due to cyclotron resonance with the anisotropic ring current H^+ ions. The energy of the excited wave is efficiently converted into the perpendicular heating of the O^+ ions thus making it more anisotropic during the main phase of the magnetic storm.

Here, we study the obliquely propagating low-frequency quasi-electrostatic waves generated by the anisotropic oxygen ions. The plasma is considered to be consisting of Maxwellian distributed electrons, and protons and energetic oxygen ions having Dory–Guest–Harris (DGH) type distribution (Dory et al. 1965; Coroniti et al. 1972; Lakhina 1976). Electrons and protons are treated as magnetized and ions as unmagnetized. The response of the electrons is fully electromagnetic, while protons and oxygen ions are considered electrostatic. In the next section, we present the theoretical model.

2. Theoretical analysis

We consider a three-component plasma consisting of Maxwellian distributed electrons with density N_e and temperature T_e, protons with density N_p and temperature T_p, and DGH-type distributed (Dory et al. 1965; Coroniti et al. 1972; Lakhina 1976) oxygen ions given by

$$f_o = \frac{N_o}{\pi^{3/2}} \frac{1}{J! \alpha_o^3} \left(\frac{v_\perp}{\alpha_o} \right)^{2J} \exp \left[- \frac{v_\perp^2 + v_\parallel^2}{\alpha_o^2} \right], \tag{1}$$

https://doi.org/10.1017/S0022377804002892 Published online by Cambridge University Press

where

$$J = \left(\frac{T_{\perp o}}{T_{\parallel o}} - 1\right)$$

which defines the temperature anisotropy, N_o, $T_{\parallel o}$, and $T_{\perp o}$ are the density, parallel and perpendicular temperatures of the oxygen ions, and $\alpha_o = \sqrt{2T_{\parallel o}/m_o}$ is the parallel thermal velocity of the oxygen ions. However, for simplicity, we have considered the proton distributions to be Maxwellian to study the instability driven by oxygen ion distributions alone. We treat electrons and protons as magnetized and oxygen ions as unmagnetized, i.e. $\omega_{co} < \omega < \omega_{cp} \ll \omega_{ce}$. The response of the electrons is fully electromagnetic, i.e. $\omega_{pe}^2/c^2k^2 \gg 1$, while protons and oxygen ions are considered to be electrostatic, i.e. $\omega_{pp}^2/c^2k^2 \ll 1$ and $\omega_{po}^2/c^2k^2 \ll 1$. Thus, under the above assumptions, a dispersion relation for the low-frequency waves propagating obliquely to the magnetic field $\mathbf{B}_0 \parallel \mathbf{z}$ can be obtained by solving the linearized Vlasov equation along with Maxwell's equations and is written as (Coroniti et al. 1972; Davidson et al. 1977; Bhatia and Lakhina 1977, 1980)

$$1 + \frac{\omega_{pe}^2}{\omega_{ce}^2}\left[\frac{1 - I_0(\lambda_e)e^{-\lambda_e}}{\lambda_e}\right] + \frac{\omega_{pe}^2}{\omega_{ce}^2}\frac{\omega_{pe}^2}{c^2k^2}\left[\frac{[\{I_0(\lambda_e) - I_1(\lambda_e)\}e^{-\lambda_e}]^2}{1 + \beta_e\{I_0(\lambda_e) - I_1(\lambda_e)\}e^{-\lambda_e}}\right]$$
$$- \frac{k_\parallel^2}{k_\perp^2}\frac{\omega_{pe}^2}{\omega^2}\frac{I_0(\lambda_e)e^{-\lambda_e}}{1 + (\omega_{pe}^2/c^2k^2)I_0(\lambda_e)e^{-\lambda_e}} - \sum_{n=1}^{\infty}\frac{4n^2\omega_{pp}^2\omega_{cp}^2}{k_\perp^2\alpha_p^2(\omega^2 - n^2\omega_{cp}^2)}I_n(\lambda_p)e^{-\lambda_p}$$
$$- \frac{\omega_{po}^2}{k^2\alpha_o^2}\frac{(-1)^J}{J!}\mu^J\left[\frac{d^J}{d\mu^J}\left[Z'\left(\frac{\omega}{k}\sqrt{\mu}\right)\right]\right] = 0, \tag{2}$$

where subscript s = e, p, o refers to electrons, protons and oxygen ions, respectively, and $Z'(\omega\sqrt{\mu}/k)$ refers to the derivative of the plasma dispersion function with respect to its argument, and $\omega_{ps} = (4\pi N_s e^2/m_s)^{1/2}$, $\omega_{cs} = eB_0/cm_s$, respectively, are the plasma and cyclotron frequencies of the species s; N_s and m_s are the density and mass of the species s, k is the wave number, c is the velocity of light, $\lambda_{e,p} = k_\perp^2\alpha_{e,p}^2/2\omega_{ce,p}^2$, $\mu^{-1} = \alpha_o^2 = 2T_{\parallel o}/m_o$, I_n is the modified Bessel function of order n and $\beta_e = 8\pi n_e T_e/B_0^2$. We choose $n = 1$ terms for protons as the frequency of the wave is much less than the proton cyclotron frequency, i.e. $\omega \ll \omega_{cp}$ and the contribution from the higher order terms will be very small. Expanding the plasma dispersion function for the oxygen ions in the limit $\omega\sqrt{\mu}/k \leqslant 1$ so as to take the effect of resonant oxygen ions, taking $n = 1$ terms for the protons in the above dispersion relation (2), and substituting for $\omega = \omega_r + i\gamma$; $\gamma \ll \omega_r$, we obtain an expression for real frequency ω_r and growth rate γ given by

$$\omega_r^2 = \frac{B \pm \sqrt{B^2 - 4C}}{2}, \tag{3}$$

$$\gamma \simeq -\frac{\sqrt{\pi}}{P}\frac{\omega_r^2\omega_{po}^2}{\alpha_o^3k^3}\left[\frac{(-1)^J}{J!}\mu^{J-1/2}\frac{d^J}{d\mu^J}\{\mu^{1/2}e^{-\mu(\omega_r^2/k^2)}\}\right], \tag{4}$$

where

$$B = \omega_{cp}^2 + \frac{\omega_{pe}^2}{P}\frac{k_\parallel^2}{k_\perp^2}\left\{\frac{I_0(\lambda_e)e^{-\lambda_e}}{1 + (\omega_{pe}^2/c^2k^2)I_0(\lambda_e)e^{-\lambda_e}}\right\} + \frac{4}{P}\frac{\omega_{cp}^2\omega_{pp}^2}{k_\perp^2\alpha_p^2}I_1(\lambda_p)e^{-\lambda_p},$$

$$C = \omega_{pe}^2\omega_{cp}^2\frac{1}{P}\frac{k_\parallel^2}{k^2}\left[\frac{I_0(\lambda_e)e^{-\lambda_e}}{1 + (\omega_{pe}^2/c^2k^2)I_0(\lambda_e)e^{-\lambda_e}}\right]$$

https://doi.org/10.1017/S0022377804002892 Published online by Cambridge University Press

and

$$P \simeq 1 + \frac{\omega_{pe}^2}{\omega_{ce}^2}\left[\frac{1 - I_0(\lambda_e)e^{-\lambda_e}}{\lambda_e}\right] + \frac{\omega_{pe}^2}{\omega_{ce}^2}\frac{\omega_{pe}^2}{c^2k^2}\left[\frac{[\{I_0(\lambda_e) - I_1(\lambda_e)\}e^{-\lambda_e}]^2}{1 + \beta_e\{I_0(\lambda_e) - I_1(\lambda_e)\}e^{-\lambda_e}}\right] + \frac{2\omega_{po}^2}{k^2\alpha_o^2}\frac{(-1)^J}{J!}\mu^J\sigma, \tag{5}$$

where $\sigma = 1$ for $J = 0$ and $\sigma = 0$ for $J \geqslant 1$. It can be seen from the growth rate expression (4), that for $J = 0$, i.e. when the perpendicular and parallel temperatures of oxygen ions are equal and hence there is no anisotropy, the growth rate is negative and waves are damped. This is expected as there is no source of free energy to drive the waves unstable. The growth rate expression for $J = 1$ is given by

$$\gamma = \frac{\sqrt{\pi}}{2P}\frac{\omega_r^2\omega_{po}^2}{\alpha_o^3k^3}\left[1 - \frac{2\omega_r^2}{k^2\alpha_o^2}\right]e^{-\omega_r^2/k^2\alpha_o^2}, \tag{6}$$

for $J = 2$ the growth rate is given by

$$\gamma = \frac{\sqrt{\pi}}{8P}\frac{\omega_r^2\omega_{po}^2}{\alpha_o^3k^3}\left[1 + \frac{4\omega_r^2}{k^2\alpha_o^2} - \frac{4\omega_r^4}{k^4\alpha_o^4}\right]e^{-\omega_r^2/k^2\alpha_o^2}, \tag{7}$$

and similarly for $J = 3$ the growth rate is given by

$$\gamma = \frac{\sqrt{\pi}}{16P}\frac{\omega_r^2\omega_{po}^2}{\alpha_o^3k^3}\left[1 + \frac{2\omega_r^2}{k^2\alpha_o^2} + \frac{4\omega_r^4}{k^4\alpha_o^4} - \frac{8}{3}\frac{\omega_r^6}{k^6\alpha_o^6}\right]e^{-\omega_r^2/k^2\alpha_o^2}. \tag{8}$$

It can be seen from the growth rate expression (6), that for the growth of the waves a condition $\omega_r^2/k^2\alpha_o^2 < \frac{1}{2}$ has to be satisfied which is consistent with our assumption used in expanding the plasma dispersion function for the oxygen ions. Now, we present the numerical results in the form of graphs and apply our results to the storm-time ring-current region. The chosen parameters for the numerical calculations for the $J = 1$ case, are $k_\parallel/k = 0.03$, $T_{\parallel o}/T_e = 20$, $T_{\parallel o}/T_p = 1$, $\omega_{pe}/\omega_{ce} = 4$, $T_e = 1\,\text{keV}$, $N_e = 10\,\text{cm}^{-3}$ and $\alpha_o/c \simeq 1.63 \times 10^{-3}$, which are representative of the storm-time ring-current region and have been used for all the calculations presented in this paper.

Figure 1 shows the variation of normalized growth rate γ/ω_{co} with $\lambda_o = k_\perp^2\alpha_o^2/2\omega_{co}^2$ for various values of the fractional oxygen ion density N_o/N_e as shown on the curves. Here, λ_o is effectively the square of the transverse wave number normalized with respect to the oxygen ion Larmor radius with parallel oxygen ion temperature. It can be seen from the figure that the growth rate increases with the increase in the fractional density of the oxygen ions. The corresponding normalized real frequency ω_r/ω_{co} is plotted in Fig. 2. It can be observed that the real frequency shows very little increase with the increase of oxygen ion concentration which is not visible on the scale of this plot. Further, in this as well as in all the following figures, the plots are cut-off at $\omega_r \simeq 10\omega_{co}$.

Figure 3 shows the variation of the normalized growth rate with $k_\parallel/k$ for various values of λ_o as indicated on the curves. Other parameters are the same as listed above and $N_o/N_e = 0.3$ for this figure and subsequent figures. It is observed that the peak growth rate increases with the increase in λ_o values. However, the range of angles of propagation for which the low-frequency waves are unstable reduces with the increase of λ_o, with peak growth shifting to lower values of $k_\parallel/k$.

https://doi.org/10.1017/S0022377804002892 Published online by Cambridge University Press

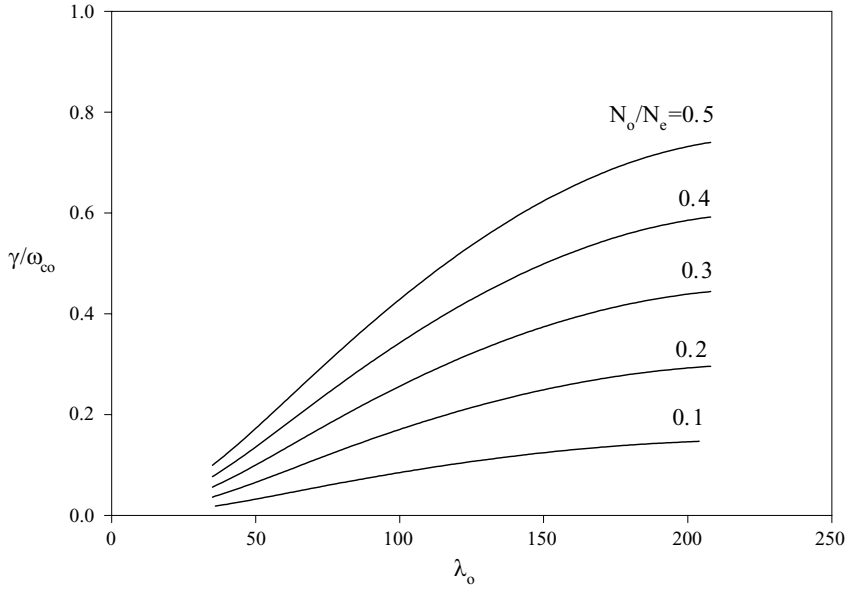

Figure 1. The variation of normalized growth rate γ/ω_{co} with λ_o for various values of the fractional oxygen ion density N_o/N_e as shown on the curves. The typical parameters are $k_\parallel/k = 0.03$, $T_{\parallel o}/T_e = 20$, $T_{\parallel o}/T_p = 1$, $\omega_{pe}/\omega_{ce} = 4$ and $\alpha_o/c \simeq 1.63 \times 10^{-3}$ for $J = 1$.

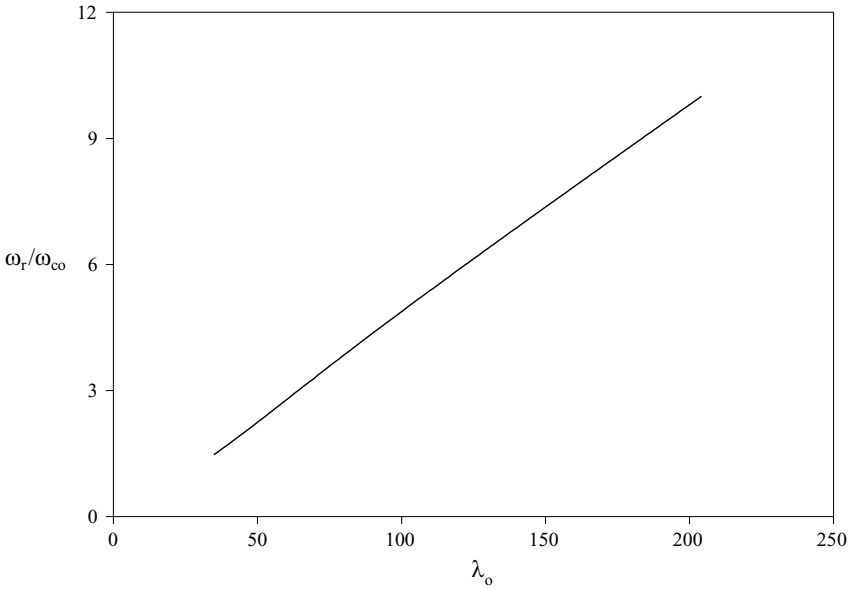

Figure 2. The normalized real frequency ω_r/ω_{co} versus λ_o for $J = 1$ for the fractional oxygen ion concentration $N_o/N_e = 0.3$. The change of N_o/N_e parameter has very little effect on the normalized real frequency. Other parameters are the same as in Fig. 1.

Figure 4 describes the variation of normalized growth rate with λ_o for same parameters as given earlier for various values of ω_{pe}/ω_{ce} as shown on the respective curves. The growth rate is higher for the smaller ω_{pe}/ω_{ce} values, i.e. the smaller the

https://doi.org/10.1017/S0022377804002892 Published online by Cambridge University Press

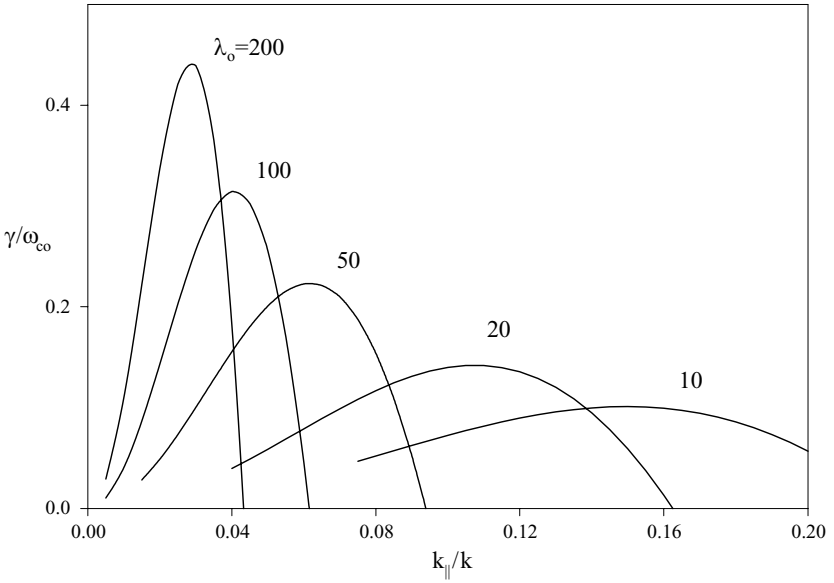

Figure 3. The variation of the normalized growth rate with $k_\parallel/k$ for $J = 1$, $N_o/N_e = 0.3$ for various values of λ_o as indicated on the curves. Other parameters are the same as in Fig. 1.

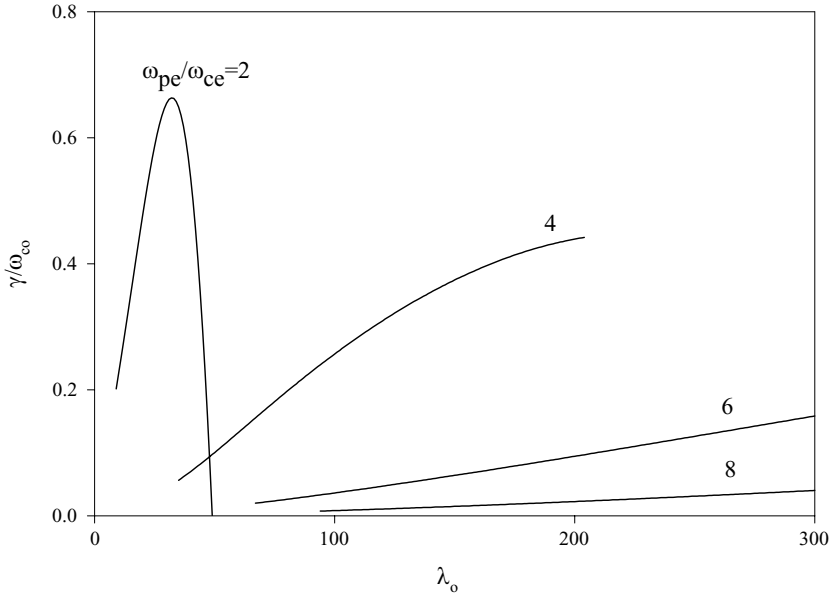

Figure 4. The variation of normalized growth rate with λ_o for $N_o/N_e = 0.3$ for various values of ω_{pe}/ω_{ce} as shown on the respective curves. Other parameters are the same as in Fig. 1.

magnetic field, the smaller the growth rate for the fixed oxygen ion concentration. Also, the range of unstable wave numbers increases with the increase in ω_{pe}/ω_{ce} values.

In Fig. 5, we plot the normalized growth rate versus λ_o for various values of the proton to oxygen ion parallel temperature ratio, i.e. $T_p/T_{\parallel o}$ as shown on the curves.

https://doi.org/10.1017/S0022377804002892 Published online by Cambridge University Press

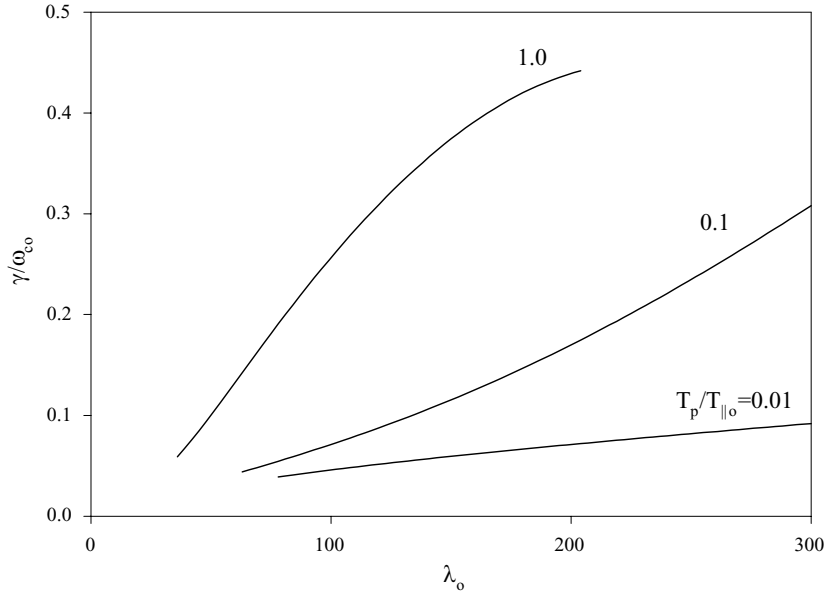

Figure 5. The normalized growth rate versus λ_o for $N_o/N_e = 0.3$ for various values of the proton to oxygen ion parallel temperature ratio, i.e. $T_p/T_{\|o}$ as shown on the curves for the parameters of Fig. 1.

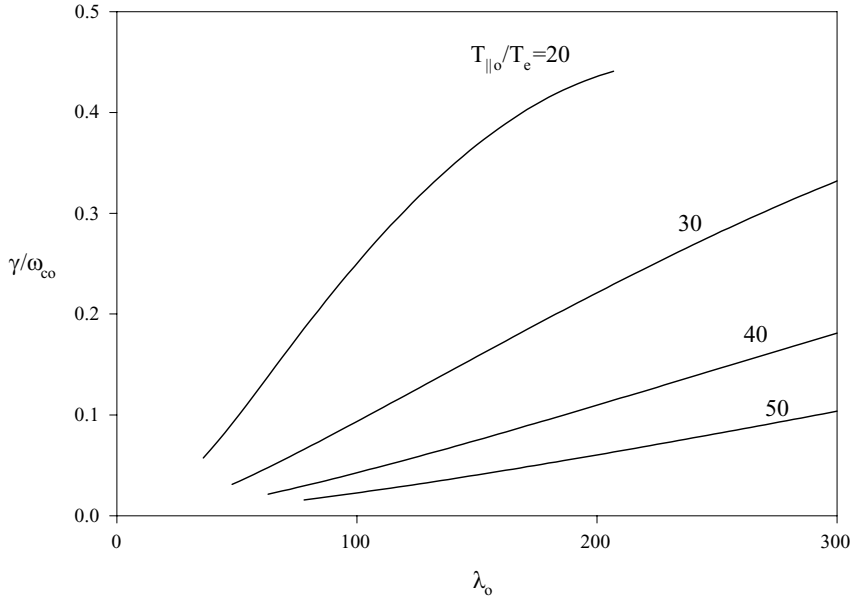

Figure 6. The normalized growth rate versus λ_o for $N_o/N_e = 0.3$ for various values of the ratio of parallel oxygen ion to electron temperature, i.e. $T_{\|o}/T_e$ as shown on the curves for the parameters of Fig. 1.

The growth rate is larger for large $T_p/T_{\|o}$ values. However, the range of unstable wave number decreases with the increase of $T_p/T_{\|o}$ values. In Fig. 6, we show the variation of parallel oxygen ion to electron temperature ratio ($T_{\|o}/T_e$). It can be

https://doi.org/10.1017/S0022377804002892 Published online by Cambridge University Press

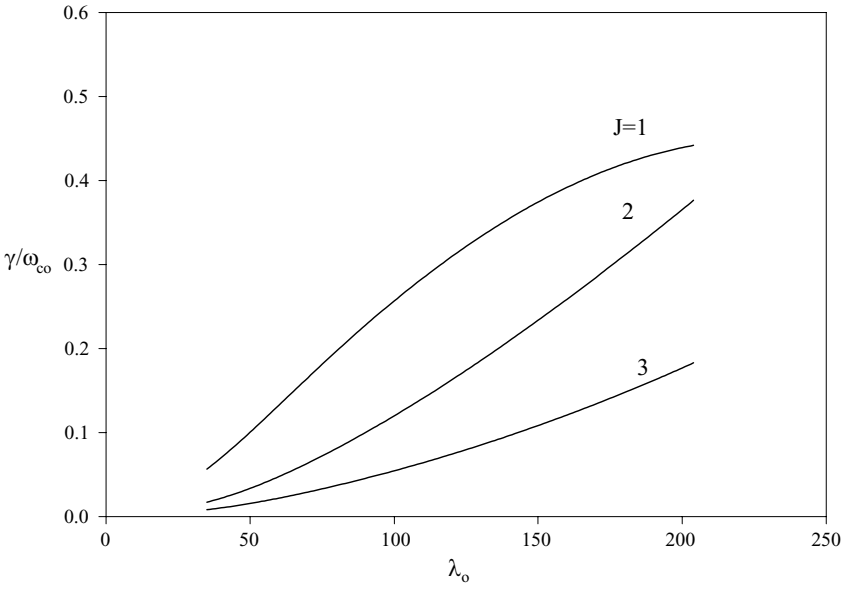

Figure 7. The comparison of the growth rates for $J = 1, 2$ and 3 for $N_o/N_e = 0.3$. Other parameters are the same as for Fig. 1.

seen from the figure that the growth rate of the low-frequency waves decreases with the increase in $T_{\parallel o}/T_e$ values, but the range of unstable wave numbers increases.

In Fig. 7, we show the comparison of the growth rates for $J = 1, 2$ and 3 values of the temperature anisotropies for the above-mentioned parameters. It can be seen from the figure that the growth rate decreases with the increase of the anisotropy. We have truncated the curves before they could attain the peak value because of the assumption of $\omega < \omega_{cp}$. Within this limitation it seems that the growth rates for higher J are smaller. It is emphasized that the behaviour of the curves shown in the Figs 1–7 is for the range of chosen parameters considered here and within the approximations of the model.

3. Application to ring current plasmas

Low-frequency instabilities generated by the anisotropic oxygen ions have been studied. It may be applied to both laboratory and space plasmas, where these loss-cone types of heavy ion distributions are observed. Here we apply our results to the storm-time ring-current region. We presented an estimate of saturation electric fields and diffusion times for different anisotropic indexes J.

Thorne and Horne (1997) have provided the Maxwellian fits to the energetic H^+ and O^+ ion distributions obtained from the ring-current atmosphere interaction model (RAM) and have given equatorial parameters. We have carried out the numerical calculations of the growth rate, real frequency, etc., for the three different values of anisotropic index J for the storm-time ring-current parameters. For $J = 1$, 2 and 3, the growth rate $\gamma \approx (10\text{–}150)$ mHz, (5–125) mHz and (2–60) mHz, respectively, as shown in Fig. 7. The real frequency and perpendicular wavelength of these low-frequency waves for the above J values are in the range $\omega_r \approx (0.4\text{–}4)$ Hz and $\lambda_\perp \approx (75\text{–}180)$ km, respectively.

https://doi.org/10.1017/S0022377804002892 Published online by Cambridge University Press

An estimate of the saturation electric field amplitude of the waves can be made by comparing the linear wave growth rate γ with the trapping frequency $\omega_t = (ekE_s/m_o)^{1/2}$ of the oxygen ions (Coroniti et al. 1972). Thus, assuming that the modes are stabilized by the trapping of O^+ ions by the waves when their amplitude becomes large, the saturation electric field (E_s) for the low-frequency waves is given by

$$E_s \simeq \frac{m_o}{e}\frac{\gamma^2}{k}. \tag{9}$$

Substituting for γ from (4) into (9), we obtain

$$E_s = \frac{\pi m_o \omega_r^4 \omega_{po}^4}{e\alpha_o^6 k^7 P^2}\left[\frac{(-1)^J \mu^{J-1/2}}{J!}\frac{d^J}{d\mu^J}\left\{\sqrt{\mu}\exp\left(-\frac{\omega_r^2}{k^2}\mu\right)\right\}\right]^2. \tag{10}$$

To estimate the diffusion time for an oxygen ion to reach the loss cone, we construct a diffusion coefficient, D given by

$$D = (\triangle v_\perp)^2/2\triangle t, \tag{11}$$

where $\triangle v_\perp = eE_s\triangle t/m_o$ and $\triangle t$ is the wave particle correlation time. Since $\gamma \sim (ekE_s/m_o)^{1/2}$ and assuming $\triangle t \approx \gamma^{-1}$, D is then given by

$$D = \frac{\gamma^3}{2k^2}. \tag{12}$$

The saturation electric fields for $J = 1, 2$ and 3 as calculated from (10) are $\simeq 60\,\mu V\,m^{-1}$ to $1.6\,mV\,m^{-1}$, $5\,\mu V\,m^{-1}$ to $1.2\,mV\,m^{-1}$ and $1.2\,\mu V\,m^{-1}$ to $0.3\,mV\,m^{-1}$, respectively, and the corresponding diffusion coefficients as calculated from (12) are of the order of $(6 \times 10^9$–$5 \times 10^{11})\,cm^2\,s^{-3}$, $(1.7 \times 10^8$–$3.2 \times 10^{11})\,cm^2\,s^{-3}$ and $(2 \times 10^7$–$3.6 \times 10^{11})\,cm^2\,s^{-3}$, respectively. The typical time during which an oxygen ion can diffuse into the loss cone with a velocity α_o is in the range $(10^3$–$10^7)$ s. This implies that the precipitation rate of the O^+ ions could vary over a large time scale from ~15 minutes to 100 days. Whereas 15 minutes is much shorter than the decay time of the ring current due to the charge exchange process (typically 10–16 hours), the diffusion time of 100 days is too long. This shows that only under certain conditions (where the saturation electric fields are large $\sim mV\,m^{-1}$) and localized regions could the ring current decay due to scattering by electrostatic waves compete with the charge exchange process.

4. Conclusion

Our results show that it is possible to excite the low-frequency quasi-electrostatic wave with anisotropic oxygen ions. The frequency of these waves is found to be between the oxygen ion and proton cyclotron frequencies. These waves have larger growth rates for nearly perpendicular propagation. Both the growth rate and real frequency are found to be increasing with the increase in the fractional oxygen ion concentration. It is also found that growth rate is higher in the region where the plasma frequency of the oxygen ions is larger than the oxygen ion cyclotron frequency. It is easier to excite these waves with smaller proton temperatures than the oxygen ion parallel temperature. The results are not significantly affected by the presence of thermal electrons. Low-frequency waves with higher anisotropy of oxygen ions will have a higher growth rate and the corresponding real frequency is not affected by the anisotropy. The growth time of these waves is a few tens of

https://doi.org/10.1017/S0022377804002892 Published online by Cambridge University Press

seconds, whereas the geomagnetic storm main phase lasts for several hours. The low-frequency waves may scatter the ring-current particles into the loss cone leading to their precipitation in the ionosphere. The ring current will be depleted due to the loss of these particles. The charge exchange of ring-current ions with neutral hydrogen has been proposed as a main mechanism for the ring current decay (Fok et al. 1995; Chen et al. 1997; Daglis et al. 1999; Ebihara and Ejiri 1999). Kozyra et al. (1997) have shown that the scattering of protons by electromagnetic ion cyclotron waves can contribute to the ring current decay. For the first time, it was shown here that the scattering of ring current particles by the low-frequency electrostatic waves could also lead to the ring current decay, thus providing a mechanism that is complimentary to the charge exchange.

References

Anderson, R. R. and Gurnett, D. A. 1973 *J. Geophys. Res.* **78**, 4756.

Anderson, B. J., Takahashi, K., Erlandson, R. E. and Zanetti, L. J. 1990 *Geophys. Res. Lett.* **17**, 1853.

Anderson, B. J., Erlandson, R. E. and Zanetti, L. J. 1992a *J. Geophys. Res.* **97**, 3075.

Anderson, B. J., Erlandson, R. E. and Zanetti, L. J. 1992b *J. Geophys. Res.*, **97**, 3089.

Bernstein, W., Hultqvist, B. and Borg, H. 1974 *Planet. Space Sci.* **22**, 767.

Bhatia, K. G. and Lakhina, G. S. 1977 *Planet. Space Sci.* **25**, 833.

Bhatia, K. G. and Lakhina, G. S. 1980 *Astrophys. Space Sci.* **68**, 175.

Chen, J. and Fritz, T. A. 2001 *Geophys. Res. Lett.* **28**, 1459.

Chen, M. W., Schulz, M. and Lyons, L. R. 1997 *Geophysics Monographs Series*, Vol. 98 (ed. B. T. Tsurutani, W. D. Gonzalez, Y. Kamide and J. K. Arballo). Washington, DC: American Geophysical Union, pp. 173.

Coroniti, F. V., Fredricks, R. W. and White, R. 1972 *J. Geophys. Res.* **77**, 6243.

Daglis, I. A. 1997 *Geophysics Monographs Series*, Vol. 98 (ed. B. T. Tsurutani, W. D. Gonzalez, Y. Kamide and J. K. Arballo), p. 107.

Daglis, I. A., Thorne, R. M., Baumjohann, W. and Orsini, S. 1999 *Rev. Geophys.* **37**, 407.

Daglis, I. A., Livi, S., Sarris, E. T. and Wilken, B. 1994 *J. Geophys. Res.* **99**, 5691.

Daglis, I. A., Kamide, Y., Mouikis, C., Reeves, G. D., Sarris, E. T., Shiokawa K. and Wilken, B. 2000 *Adv. Space Res.* **25**, 2369.

Davidson, R. C., Gladd, N. T., Wu, C. S. and Huba, J. D. 1977 *Phys. Fluids*, **20**, 301.

Dory, R. A., Guest, G. E. and Harris, E. G. 1965 *Phys. Rev. Lett.*, **14**, 131.

Ebihara, Y. and Ejiri, M. 1999 *Adv. Polar Upper Atmos. Res.* **13**, 1.

Fok, M.-C., Moore, T. E., Kozyra, J. U., Ho, G. C. and Hamilton, D. C. 1995 *J. Geophys. Res.* **100**, 9619.

Gorney, D. J., Clarke, A. C., Croley, D., Fennell, J., Luhmann, J. and Mizera, P. 1981 *J. Geophys. Res.* **86**, 83.

Gurnett, D. A. 1976 *J. Geophys. Res.* **81**, 2765, 1976.

Gurnett, D. A. and Frank, L. A. 1977 *J. Geophys. Res.* **82**, 1031.

Gurnett, D. A. and Frank, L. A. 1978 *J. Geophys. Res.* **83**, 1447.

Hamilton, D. C., Gloeckler, G., Ipovitch, F. M., Studenmann, W., Wilken, B. and Kremser, G. 1988 *J. Geophys. Res.* **93**, 14343.

Horne, R. B. and Thorne, R. M. 1993 *J. Geophys. Res.* **98**, 9233.

Horne, R. B. and Thorne, R. M. 1994 *J. Geophys. Res.* **99**, 17259.

Kozyra, J. U., Jordanova, V. K., Horne, R. B. and Thorne, R. M. 1997 *Geophysics Monographs Series*, Vol. 98 (ed. B.T. Tsurutani, W. D. Gonzalez, Y. Kamide and J. K. Arballo), p. 107.

Laakso, H., Junginger, H., Roux, A., Schmidt, R. and de Villedary, C. 1990 *J. Geophys. Res.* **95**, 10609.

Lakhina, G. S. 1976 *Planet. Space Sci.* **24**, 609.

Nose, M., Ohtani, S., Takahashi, K., Lui, A. T. Y., McEntire, R. W., Williams, D. J., Christon, S. P. and Yumoto, K. 2001 *J. Geophys. Res.* **106**, 8391.

Nose, M., Lui, A. T. Y., Ohtani, S., Mauk, B. H., McEntire, R. W., Williams, D. J., Mukai, T. and Yumoto, K. 2000 *J. Geophys. Res.* **105**, 7669.

Perraut, S., Roux, A., Robert, P., Gendrin, R., Sauvaud, J. A., Bosqued, J. M., Kremser, G. and Korth, A. 1982 *J. Geophys. Res.* **87**, 6219.

Peterson, W. K., Yau, A. W. and Whalen, A. B. 1993 *J. Geophys. Res.* **98**, 11177.

Putvinski, S. V. 1998 *Nucl. Fusion* **38**, 1275.

Russel, C. T., Holzer, R. E. and Smith, E. J. 1970 *J. Geophys. Res.* **75**, 755.

Sharp, R. D., Johnson, R. G. and Shelly, E. G. 1977 *J. Geophys. Res.* **82**, 3324.

Shelly, E. G., Sharp, R. D. and Johnson, R. G. 1976 *Geophys. Res. Lett.* **3**, 654.

Thorne, R. M. and Horne, R. B. 1994 *J. Geophys. Res.* **99**, 17275.

Thorne, R. M. and Horne, R. B. 1997 *J. Geophys. Res.* **102**, 14155.

Watkins, M. L. 1998 *Nucl. Fusion* **38**, 1336.